JOURNAL OF MATERIALS SCIENCE 29 (1994) 700–707

Influence of different process parameters on physical properties of fluorine doped indium oxide thin films

S. MIRZAPOUR, S. M. ROZATI, M. G. TAKWALE, B. R. MARATHE, V. G. BHIDE
School of Energy Studies, Department of Physics, University of Poona, Pune 411 007, India

Fluorine-doped indium oxide films were prepared by the spray pyrolysis technique. The physical properties of these films were investigated with respect to various process parameters, namely variation of dopant concentration (in the solution), deposition temperature (T_s), carrier gas (air) flow rate and the thickness of the film. The best films had a Hall mobility of the order of 28 $cm^2 V^{-1} s^{-1}$ and a carrier density of $2.7 \times 10^{20} cm^{-3}$. These films were deposited at $T_s = 425\,^{\circ}C$ at an air flow rate of 71 min^{-1} for an atomic ratio of flourine to indium of 72%. The electrical resistivity of these films was of the order of $10^{-4} \Omega$ cm and the average transmission in the visible range was found to be 80–90%. The films were polycrystalline, n-type semiconductors with [400] as a preferred orientation. The preferred orientation changes from [400] to [222] depending upon the process parameters.

1. Introduction

Transparent and conducting oxides (TCO) of In_2O_3, SnO_2, ZnO etc. prepared by various techniques have a wide range of applications in photovoltaic and photothermal technologies. Tin-doped indium oxides films are more commonly prepared and used as transparent conducting oxides. Only a few publications report on fluorine-doped indium oxide thin films deposited by different techniques [1–3] including spray pyrolysis [2]. The present investigations show for the first time the dependence of physical properties of spray-deposited In_2O_3:F films on air flow rate and thickness of the films.

2. Experimental procedure

Thin layers of In_2O_3:F were deposited on Corning 7059 substrates by the spray pyrolysis technique. The details of the experimental procedure are given elsewhere [4, 5]. Here we have investigated the physical properties of In_2O_3:F films with respect to four different process parameters: (i) dopant concentration, (ii) deposition temperature, (iii) air flow rate and (iv) the thickness of film. The spraying solution consisted of indium chloride and ammonium fluoride used as a dopant, where the [F]/[In] ratio was varied from 8 to 104%. The films were deposited at a substrate temperature of $T_s = 425\,^{\circ}C$ and an air flow rate of 71 min^{-1}, which happen to be our optimum values for undoped In_2O_3 films [6]. The films were deposited for a fixed time of 24 min. The optimum ratio [F]/[In] was found to be 72%. This value was kept constant when other parameters were varied. In terms of weight percentage the doping concentration varies from 1.32 to 17.2%.

The deposition temperature was varied from 350 to 500 °C for the optimum dopant level. The optimum temperature was found to be 425 °C. The air flow rate was varied from 5 to 11 1 min^{-1}, keeping the dopant concentration and substrate temperature at their optimum values. The optimum air flow rate was found to be 71 min^{-1}. The thickness of the film was varied in the range of 0.1 to 1.3 μm varying the time of deposition, other process parameters being at their optimum level. The electrical resistivity of the films was determined using the van der Pauw technique [7]. Hall mobility μ_H and carrier concentration (N) were determined by using Hall effect measurements at room temperature. A Hitachi optical spectrophotometer was used to measure the optical properties of the films. Structural properties of the films were studied by using a low angle X-ray diffractometer (Rigaku rotating anode X-ray diffractometer RU 200 B). The thickness of the films was measured by using the formula given by Manifacier and Fillard [8].

3. Results and discussion

3.1. Variation of dopant concentration

The In_2O_3:F films are found to be polycrystalline with the preferred orientation [400]. The extent of this orientation increases with doping upto a doping concentration of 72%, after which there is a decrease in this preferred orientation as seen in Fig. 1. Similar results have been observed by Maruyama and Fukui [3] in In_2O_3:F and In_2O_3:Sn films deposited by the chemical vapour deposition technique. The variation

0022–2461

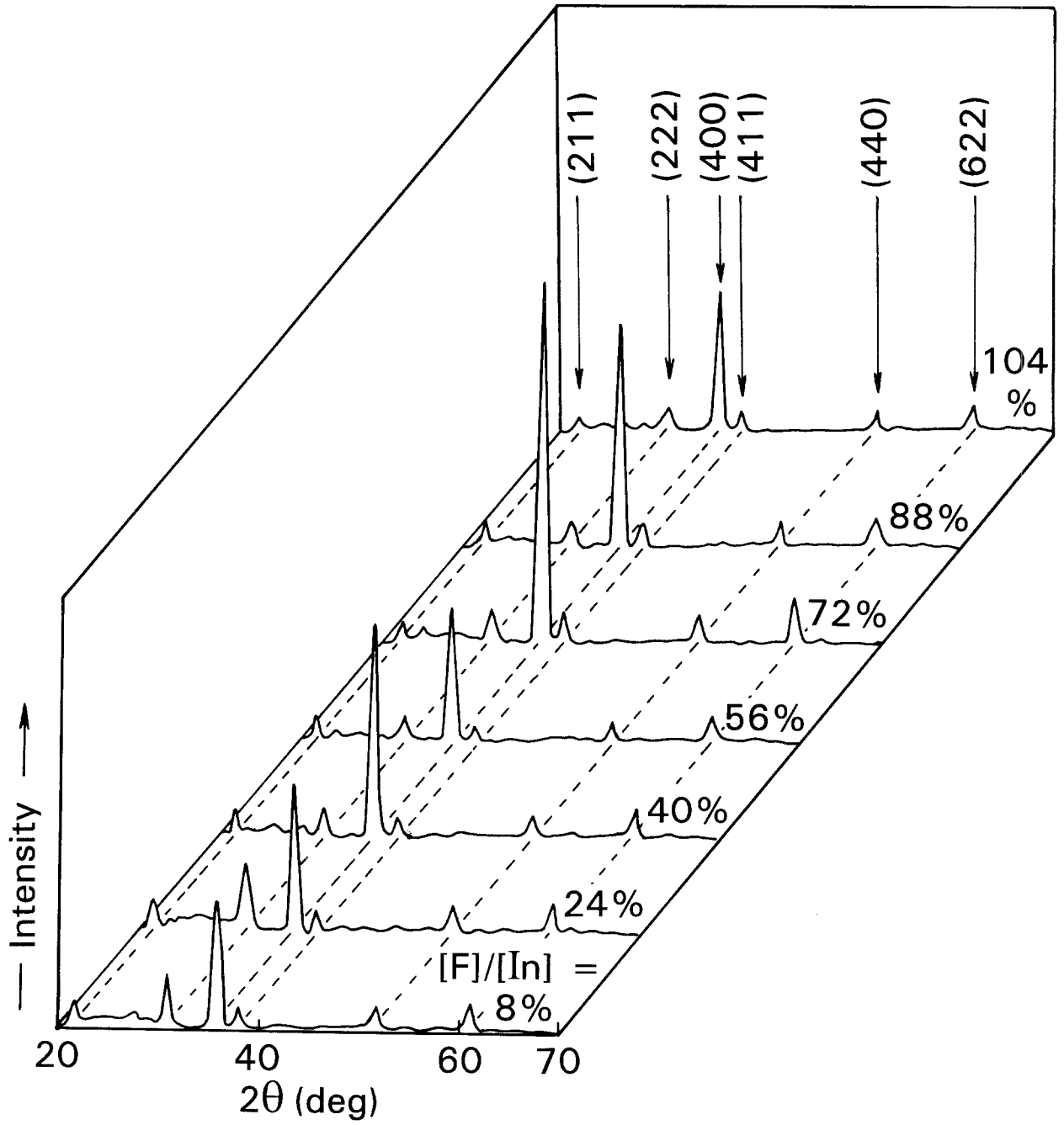

Figure 1 Variation of X-ray diffraction pattern with ratio [F]/[In]; T_s = 425 °C, flow rate = 71 min^{-1}.

of texture coefficient for [400] and [222] orientations, calculated using the formula given by Barret and Massalski [9] for different dopant concentrations, is shown in Fig. 2.

The variations of Hall mobility μ_H, carrier concentration (N) and the electrical resistivity (ρ) with doping are shown in Fig. 3. The initial decrease in N could be due to the dopant fluorine occupying oxygen vacancy sites [10]. Whereas the oxygen vacancy denotes two electrons to the lattice, replacement of the vacancy by a fluorine atom results in the donation of only one electron. A further increase in dopant concentration results in the replacement of oxygen by fluorine and thus an increase in the carrier concentration. Yuanri *et al.* [11] have also observed an initial decrease in N in In_2O_3:Sn films deposited by reactive ion planting, but no explanation has been proposed for this variation of N.

The Hall mobility μ_H appears to depend on the number of oxygen vacancies, the number of ionized impurities and the crystallinity of the films. The initial increase in μ_H could be due to the reduction in oxygen vacancies and improvement in the crystallinity. The decrease in μ_H at higher concentration appears to be due to a loss of crystallinity as well as an increase in the number of ionized impurities. The highest measured value of μ_H was 36 cm^2 V^{-1} s^{-1}.

The relation between μ_H and N was calculated using the following formula [12] and plotted in Fig 4:

$$\mu \simeq \frac{4e}{h}\left(\frac{\pi}{3}\right)^{1/3} N^{-2/3}$$

$$= 9.816 \times 10^{14} N^{-2/3} \quad (\text{cm}^2\,\text{V}^{-1}\,\text{s}^{-1})$$

The slope of the curve (Fig. 4) was 0.67, which agrees well with the value 0.8 ± 0.2 given by Hoffmann *et al.*

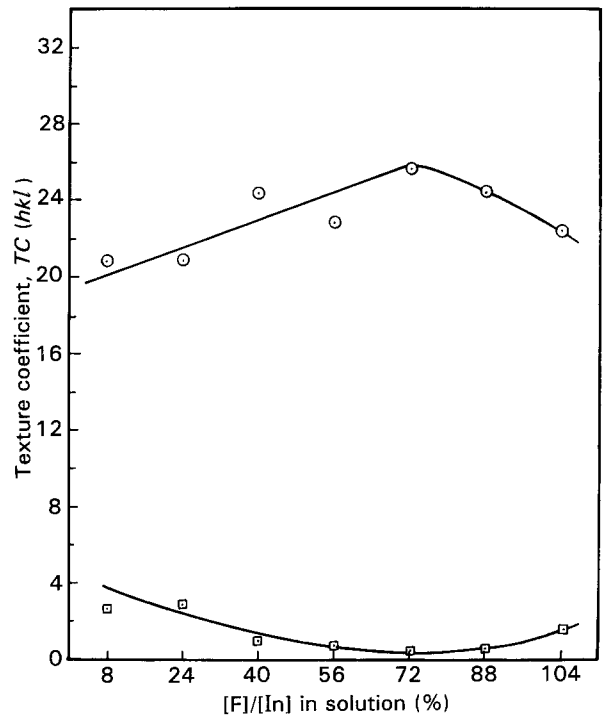

Figure 2 Variation of texture coefficient with ratio [F]/[In] for (⊙) (400), (⊡) (222).

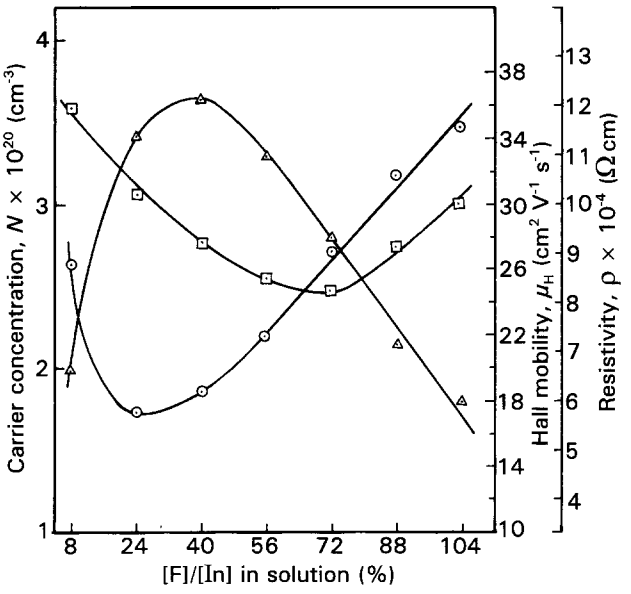

Figure 3 Variation of (△) Hall mobility μ_H, (○) carrier concentration N and (□) resistivity ρ versus doping concentration. $T_s = 425\,°C$, flow rate = 71 min^{-1}, t = 320–420 nm.

[13]. This supports the reasoning that ionized impurity scattering influences μ_H at higher doping concentrations.

Since the resistivity depends on the product of N and μ_H, it incorporates the variation of these two parameters. The minimum value of resistivity is obtained when the [F]/[In] ratio is 72%.

The effect of doping on the sheet resistance R_{sh} and the figure of merit as defined by Fraser and Cook [14] is shown in Fig. 5. On both counts, the optimum

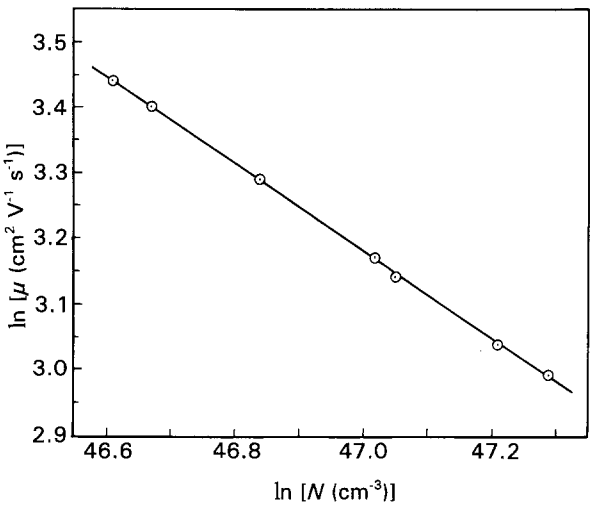

Figure 4 Variation of mobility μ with carrier concentration N: $\mu_H \propto N^{-2/3}$.

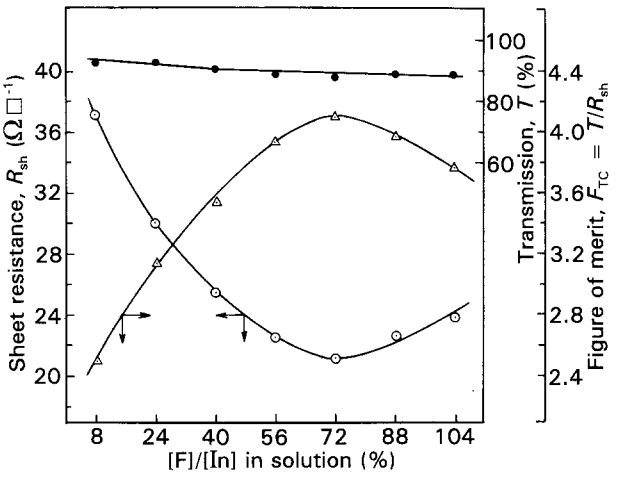

Figure 5 Variation of (○) sheet resistance R_{sh}, (●) optical transmission T and (△) figure of merit F_{TC} versus doping concentration.

doping level is an atomic fluorine to indium ratio of 72%. This corresponds to 11.90 wt % ratio of fluorine to indium. Singh *et al.* [2] observed a lower value of 2.4 wt % as the optimum doping. Whereas their range of doping studied was 1 to 5 wt %, this range is 1 to 17 wt % in the present investigation.

From the optical measurements it was observed that the films have a high transmission (87–90%) in the visible range of the spectrum. A plot of the square of absorption coefficient (α^2) against photon energy [3] as shown in Fig. 6 gives a value of 3.82 eV as the band gap of In_2O_3:F. This value is higher than the one observed by us for undoped films [6]. Maruyama and Fukui [3] find for their undoped and fluorine-doped In_2O_3 films deposited by the CVD technique a lower value of 3.50 eV as the band gap. Doping did not change their value of band gap.

3.2. Variation of substrate temperature

The substrate temperature was varied from 350 to 500 °C with an interval of 25 °C. The thickness of the

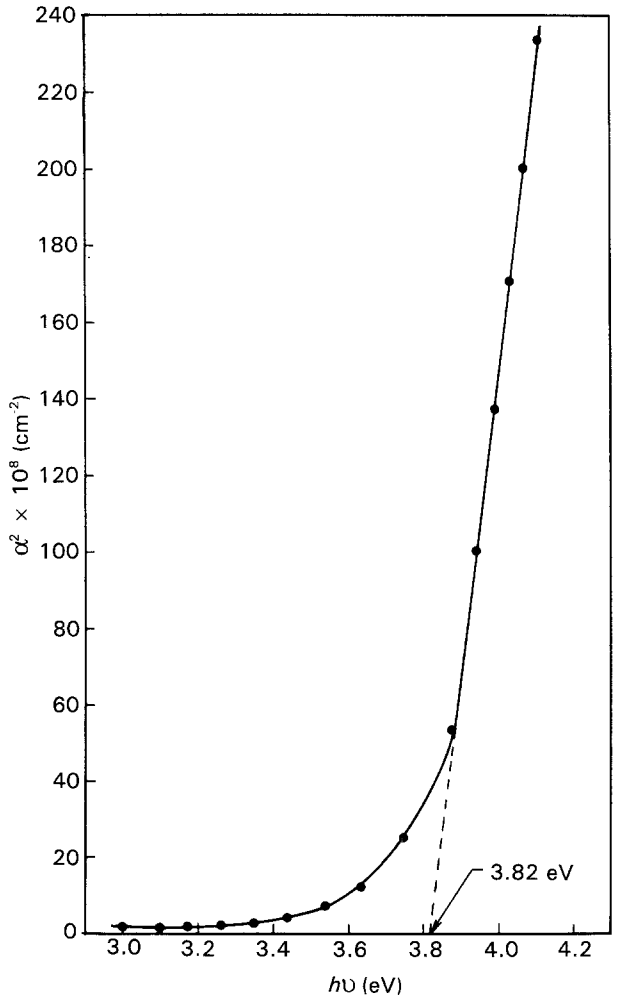

Figure 6 Square of absorption coefficient as a function of photon energy of In_2O_3:F thin films.

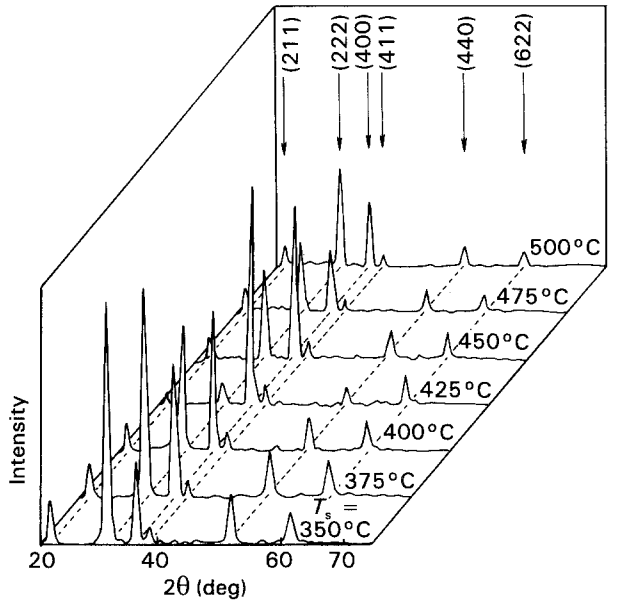

Figure 7 Variation of X-ray diffraction pattern with substrate temperature T_s; [F]/[In] = 72%, flow rate = 7 l min^{-1}.

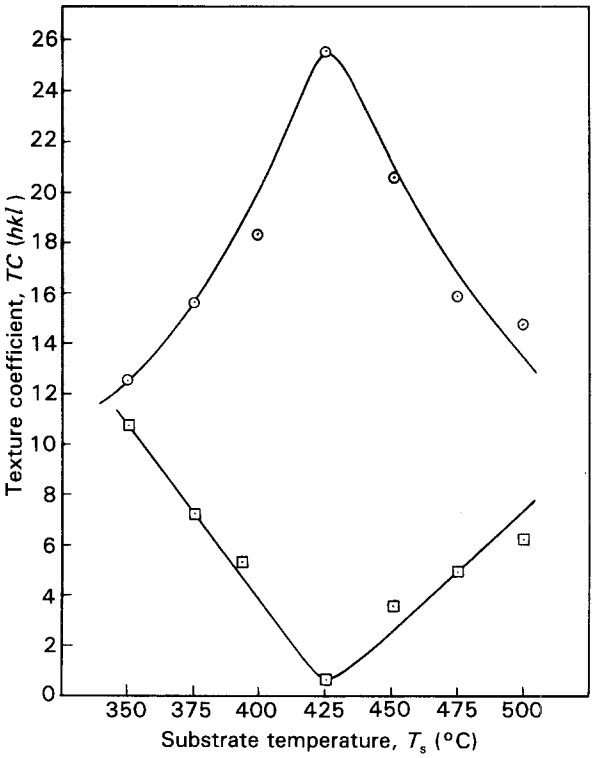

Figure 8 Variation of texture coefficient with substrate temperature for (○) (400), (□) (222).

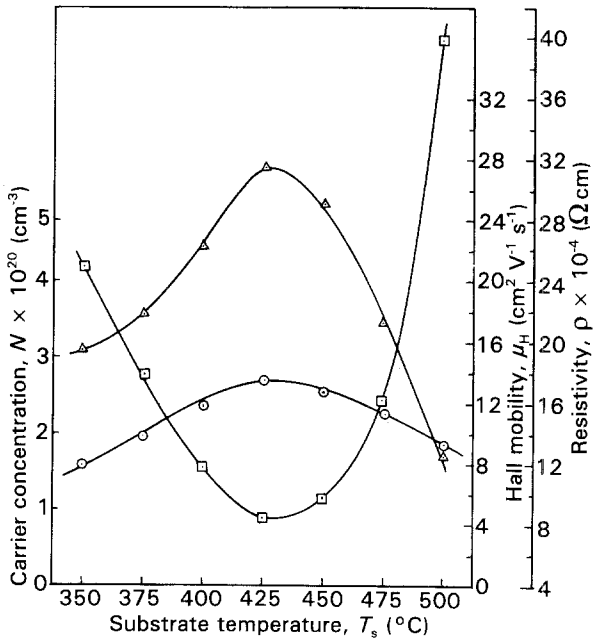

Figure 9 Effect of substrate temperature on electrical properties of spray-deposited In_2O_3:F at room temperature: (△) mobility, (□) ρ, (○) N. [F]/[In] = 72%, flow rate = 7 l min^{-1}.

film was 370–435 nm. The substrate temperature had a remarkable influence on the preferred orientation of the films, as seen from Fig. 7. Similar results were observed for undoped In_2O_3 films [6]. These and the earlier X-ray diffraction (XRD) observations suggest a minimum deposition temperature of 350 °C for obtaining In_2O_3 films. Lower temperatures show peaks of $InCl_3$ and not In_2O_3. Groth [15] and Siefert [16] have reported similar observations although Singh *et al.* [2] have deposited In_2O_3 films at a temperature as low as 310 °C. Variation in the preferred orientation with different deposition temperatures for In_2O_3:F

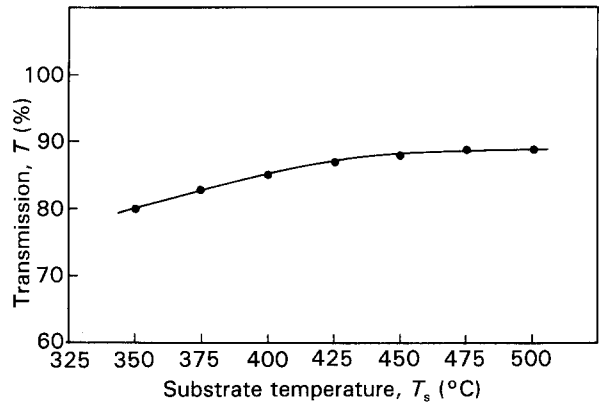

Figure 10 Variation of room-temperature optical transmission T with substrate temperature of In_2O_3:F thin film.

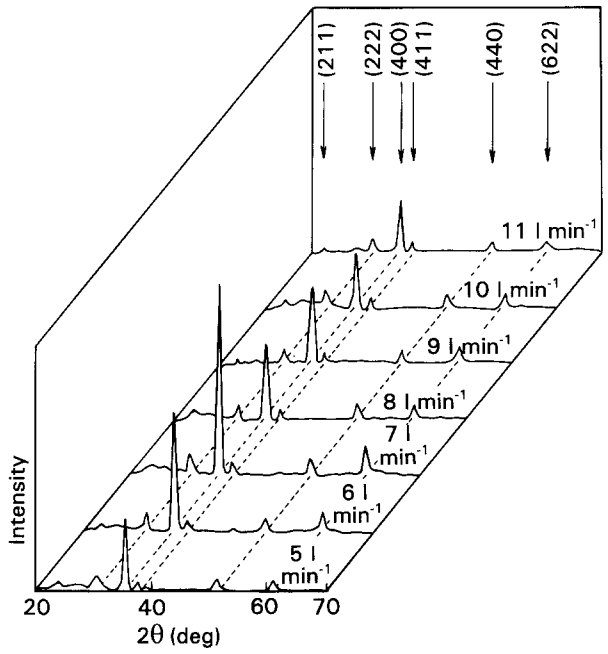

Figure 11 X-ray diffraction patterns of In_2O_3:F films deposited at different air flow rates (1 min^{-1}). T_s = 425 °C, [F]/[In] = 72%.

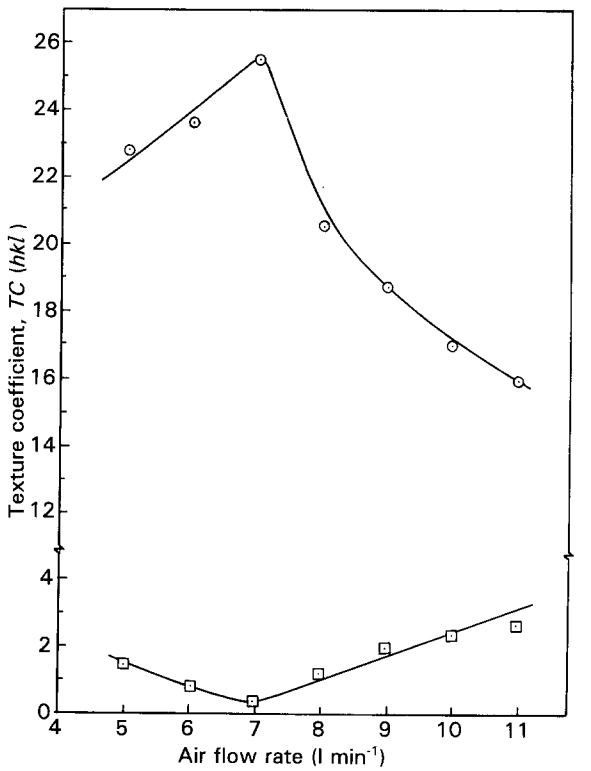

Figure 12 Texture coefficient for (○) [400] and (□) [222] at different air flow rates.

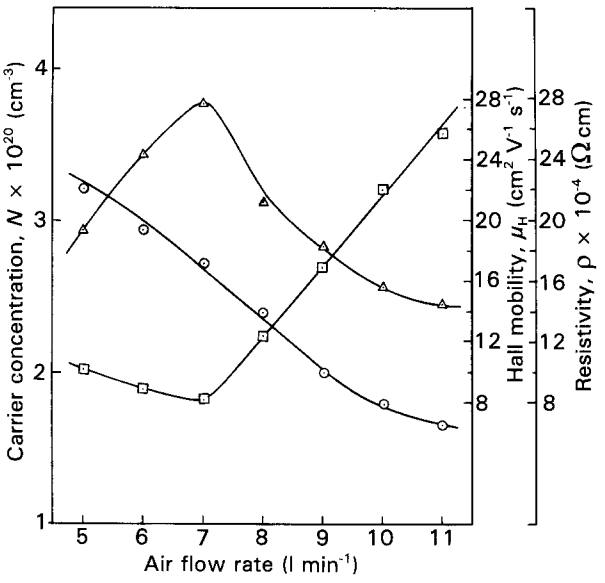

Figure 13 Effect of air flow rate on electrical properties of spray-deposited In_2O_3:F at room temperature: (△) mobility, (□) ρ, (○) N.

films has not been observed by other workers [2, 3, 17]. Fig. 8 shows the texture coefficient variation with deposition temperature for the two orientations [400] and [222].

The Hall mobility μ_H, carrier concentration N and electrical resistivity ρ of In_2O_3:F films as a function of substrate temperature are plotted in Fig. 9. Both μ_H and N follow the trend of variation of the predominant [400] orientation which may be understood as due to enhanced crystallinity with increasing substrate temperature [18]. The decrease in N at higher substrate temperatures than the optimum 425 °C could be due to reduced effectiveness of doping as a result of a decrease in crystallinity of the film. Additionally, higher deposition temperatures may reduce the contribution of oxygen vacancies to N [12]. Since both μ_H and N peak at 425 °C, the lowest resistivity of 8.3 $\times 10^{-4}\,\Omega$cm is observed at this deposition temperature. Shanthi *et al.* [19] have observed a similar behaviour of physical properties with deposition temperature. The average optical transmission in the visible region increases from 80 to 89% as the substrate temperature is increased from 350 to 500 °C (Fig. 10).

3.3. Variation of air flow rate

The structural properties of the films at different air flow rates are shown in Figs 11 and 12, while the

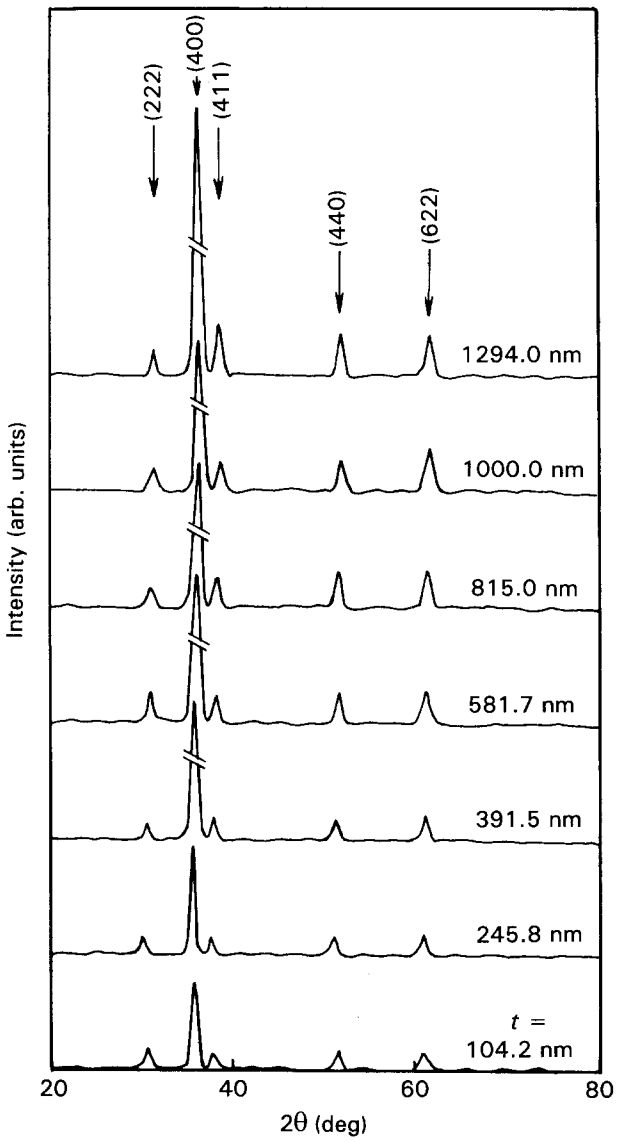

Figure 14 X-ray diffraction patterns of In_2O_3:F films of various thicknesses. T_s = 425 °C, flow rate 71 min^{-1}, [F]/[In] = 72%.

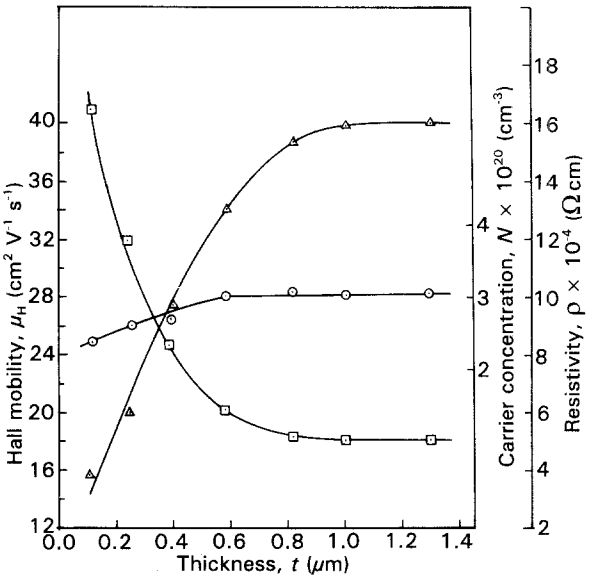

Figure 15 Effect of thickness on electrical properties of spray-deposited In_2O_3:F at room temperature: (△) mobility, (□) ρ, (○) N. T_s = 425 °C, flow rate = 71 min^{-1}, [F]/[In] = 72%.

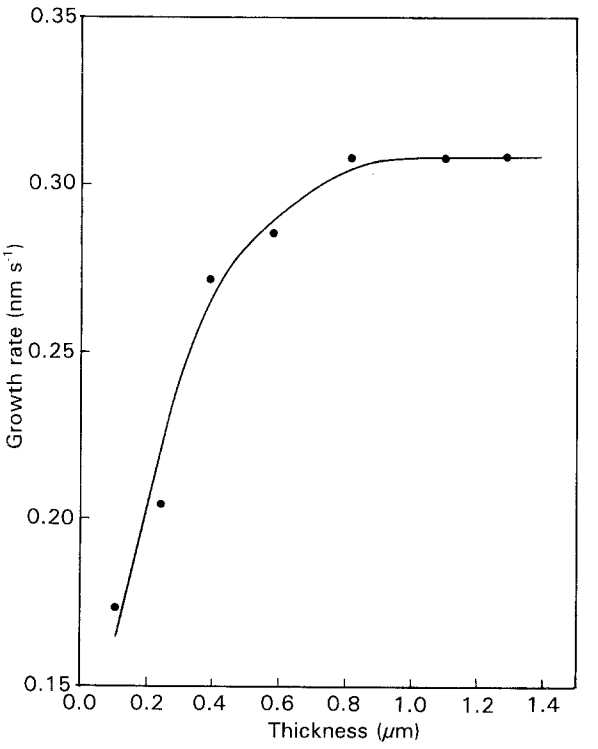

Figure 16 Variation of growth rate of In_2O_3F: films with thickness. T_s = 425 °C, flow rate 71 min^{-1}, [F]/[In] = 72%.

variation in electrical properties appears in Fig. 13. The Hall mobility μ_H is distinctly structure-dependent and follows the variation of the [400] preferential orientation. Since N results from the contribution of both oxygen vacancies and the dopant, the higher value of N at lower flow rates could possibly be due to a high number of oxygen vacancies as a result of a higher loss of oxygen at lower flow rates. As the flow rate increases the films become more stoichiometric, resulting in a reduction of N. The optimum flow rate is 71 min^{-1}.

3.4. Variation of film thickness

The extent of preferential orientation along [400] increases with thickness as seen in Fig. 14. Although we had observed a change in orientation with thickness in undoped films [20], no such change was observed in the doped films in the present investigation. Belanger and Dodelet [21], however, have observed a change in orientation for SnO_2:F and SnO_2:Sb for thicknesses above 1 μm.

The thinner films have a larger surface to volume ratio [22] and there are more defects in thin films. As the thickness increases, these defects get reduced. This would account for a lower μ_H for smaller thickness values and an increase in μ_H with higher thickness, which finally saturates for films with a thickness above 1 μm. The variation in N is small and the lower N values for thinner films could be due to reduced effective doping in these defective films. These results are shown in Fig. 15. The lowest electrical resistivity ρ is 5×10^{-4} Ωcm for a film thickness of 1 μm. The

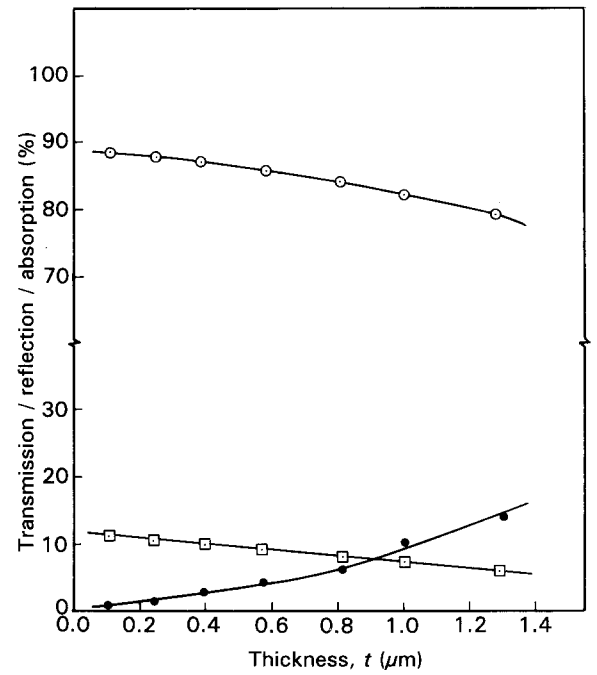

Figure 17 Variation with thickness of room-temperature (○) transmission, (□) reflection and (●) absorption of In_2O_3:F films in the visible range. T_s = 425 °C, flow rate = 7 l min^{-1}, [F]/[In] = 72%.

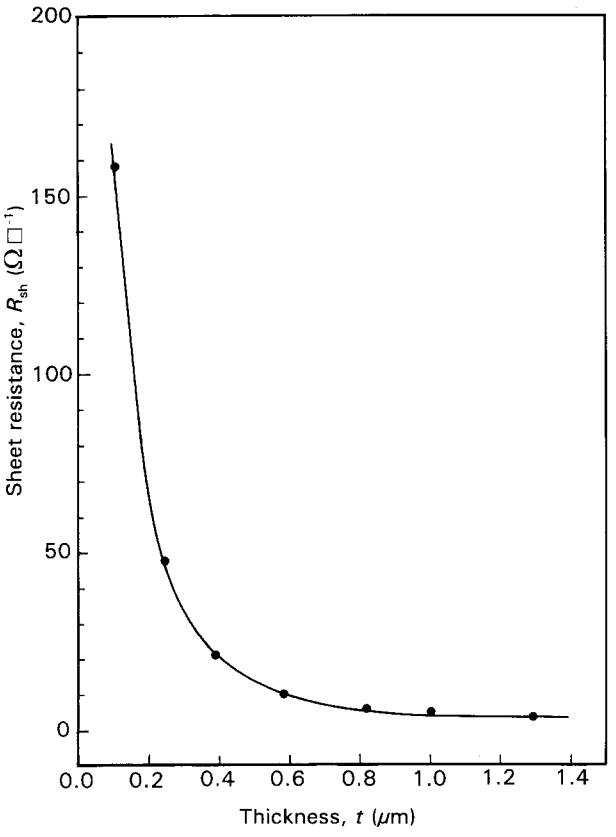

Figure 18 Variation of sheet resistance R_{sh} with thickness. T_s = 425 °C, flow rate = 7 l min^{-1}, [F]/[In] = 72%

growth rate also saturates above 0.8 μm thickness as seen in Fig. 16.

The variation of average transmission, reflection and absorption with film thickness is given in Fig. 17. The transmission is good, about 80%, even for films having a thickness of 1.3 μm.

The variation of sheet resistance with thickness is shown in Fig. 18. The lowest sheet resistance of about 4 $\Omega\,\square^{-1}$ is obtained for a film thickness of 1.3 μm.

4. Conclusion

The dependence of structural, electrical and optical properties of spray-deposited In_2O_3:F films on process parameters such as doping concentration, substrate temperature, air flow rate and thickness of the film has been studied in detail. Keeping three of the above four process parameters constant, the optimum value of the fourth parameter has been determined to give the best electrical and optical properties.

In the process of this investigation it has been observed that the films are polycrystalline and have a preferred orientation in the [4 0 0] direction. The variation in the Hall mobility μ_H is closely related to the variation in this preferred orientation. Only in some cases does the mobility appear to be dependent on other factors such as specific defects in the film (as in the case of thin films) and on the level of ionized impurities.

The carrier concentration N has contributions both from oxygen vacancies and from the dopant. As the stoichiometry improves, the contribution to N from oxygen vacancies decreases. An increase in dopant concentration should increase N but the effectiveness of doping depends on the quality of the film. This effectiveness is less for defective films. One useful parameter to evaluate the quality of the film is the XRD information. In some cases, very high doping leads to compensation of the dopant, resulting in a lowering of N.

The variation of optical properties in the present investigation has been comparatively small, unlike in tin oxide films where the different phases of this oxide influence the optical transmission. Defects in the film do contribute to a loss of optical transmission.

References

1. J. N. AVARITSIOTIS and R. P. HOWSON, *Thin Solid Films* **80** (1980) 63.
2. S. P. SINGH, A. RAZA, A. K. SHARMA, O. P. AGNIHOTRI and L. M. TEWARI *ibid.* **105** (1983) 131.
3. T. MARUYAMA and K. FUKUI, *Jpn J. Appl. Phys.* **29** (1990) L 1705.
4. S. MIRZAPOUR, S. M. ROZATI, M. G. TAKWALE, B. R. MARATHE and V. G. BHIDE, *Mater. Chem. Phys.* **33** (1993) 204.
5. E. SHANTHI, V. DUTTA, A. BANERJEE and K. L CHOPRA, *J. Appl. Phys.* **51** (1980) 6243.
6. S. MIRZAPOUR, S. M. ROZATI, M. G. TAKWALE, B. R. MARATHE and V. G. BHIDE, *Mater. Lett.* **13** (1992) 275.
7. J. L. Van der PAUW, *Philips Res. Rep.* **13** (1958) l.
8. J. C. MANIFACIER and J. P. FILLARD, *Thin Solid Films* **77** (1981) 67.
9. C. BARRET and T. B. MASSALSKI, in "Structure of Metals" (Pergamon, Oxford, 1980) p. 204
10. H. de WAAL and F. SIMONIS, *Thin Solid Films* **77** (1981) 253.
11. C. YUANRI, X. XINGHAO, J. ZHAOTING, P. CHUANCAI and X. SHUYUN, *ibid.* **115** (1984) 195.
12. S. NOGUCHI and H. SAKATA, *J. Phys. D* **13** (1980) 1129.
13. H. HOFFMANN, J. PICKL, M. SCHMIDT and D. KRAUSE *Appl. Phys.* **16** (1978) 239.

14. D. B. FRASER and H. D. COOK, *J. Electrochem. Soc.* **119** (1972) 1368.
15. R. GROTH, *Phys. Status Solidi* **14** (1966) 69.
16. W. SIEFERT, *Thin Solid Films* **121** (1984) 275.
17. J. N. AVARITSIOTIS and R. P. HOWSON, *ibid.* **77** (1981) 351.
18. N. BALASUBRAMANIAN and A. SUBRAHMANYAM, *J. Phys. D* **22** (1989) 206.
19. E. SHANTHI, A. BANERJEE, V. DUTTA and K. L. CHOPRA, *J. Appl. Phys.* **53** (1982) 1615.
20. S. MIRZAPOUR, S. M. ROZATI, M. G. TAKWALE, B. R. MARATHE and V. G. BHIDE, *Mater. Res. Bull.* **27** (1992) 133.
21. D. BELANGER and J. P. DODELET, *J. Electrochem. Soc.* **132** (1985) 1398.
22. A. K. SAXENA, S. P. SINGH, R. THANGARAJ and O. P. AGNIHOTRI, *Thin Solid Films* **117** (1984) 95.

Received 24 August 1992
and accepted 9 August 1993